

Linear Orbit Correction in the AGS to RHIC Transfer Lines

T. Satogata

April 1994

Collider Accelerator Department
Brookhaven National Laboratory

U.S. Department of Energy

USDOE Office of Science (SC)

Notice: This technical note has been authored by employees of Brookhaven Science Associates, LLC under Contract No. DE-AC02-76CH00016 with the U.S. Department of Energy. The publisher by accepting the technical note for publication acknowledges that the United States Government retains a non-exclusive, paid-up, irrevocable, world-wide license to publish or reproduce the published form of this technical note, or allow others to do so, for United States Government purposes.

DISCLAIMER

This report was prepared as an account of work sponsored by an agency of the United States Government. Neither the United States Government nor any agency thereof, nor any of their employees, nor any of their contractors, subcontractors, or their employees, makes any warranty, express or implied, or assumes any legal liability or responsibility for the accuracy, completeness, or any third party's use or the results of such use of any information, apparatus, product, or process disclosed, or represents that its use would not infringe privately owned rights. Reference herein to any specific commercial product, process, or service by trade name, trademark, manufacturer, or otherwise, does not necessarily constitute or imply its endorsement, recommendation, or favoring by the United States Government or any agency thereof or its contractors or subcontractors. The views and opinions of authors expressed herein do not necessarily state or reflect those of the United States Government or any agency thereof.

Linear Orbit Correction in the AGS to RHIC Transfer Lines

T. Satogata

I. Introduction and Transfer Line Linear Correction System Layout

The AGS to RHIC transfer lines each cover a distance of approximately 600 meters, with phase advances of approximately 11π radians in each plane. There are many vertical aperture restrictions present (mostly concentrated in the combined-function dipoles of the various bends), as well as a vertical pitch through the W line that makes these transfer lines non-planar. This investigation has several objectives, of which only one is reported on here. This is specifically to determine whether the linear orbit may be corrected to within one beam sigma in both planes, even with any single bpm or dipole corrector broken; more generally, where is the linear orbit correction in the AGS to RHIC transfer line best and where is it worst? The quantitative criterion may at first seem too stringent, but it must be stressed that adequate and robust linear orbit correction and optical matching in any transfer line are crucial for efficient beam transfer and flexibility of operation.

At the injection rigidity of $B\rho = 97.5 \text{ T-m}$ for beam extracted from the AGS, the sizes of gold and proton beams with typical emittances of $15\pi \text{ mm-mrad}$ and $10\pi \text{ mm-mrad}$, respectively, are

$$\begin{aligned}\sigma(p) &= 0.2833 \text{ mm} \sqrt{\beta[\text{m}]}, \\ \sigma(\text{Au}) &= 0.3639 \text{ mm} \sqrt{\beta[\text{m}]},\end{aligned}\tag{1}$$

where β is the beta function at the observation point. β varies from about 4.5 m (U-line quad 10) to 175 m (U-line quad 9) in the horizontal plane, and from about 4 m (AGS extraction) to 100 m (U-line quad 4) in the vertical; in the X and Y 90 degree bends where vertical aperture is a serious consideration, the maximum betas are approximately 30 m. At these points the vertical aperture is $14.35 \text{ mm} = 9.25\sigma(p) = 7.20\sigma(\text{Au})$. The horizontal and vertical physical apertures are plotted in Figure (1), showing the vertical aperture restrictions of 14 to 17 mm in each of the major bends — eight degree, twenty degree and ninety degree. The horizontal aperture can be considered to be 39.37 mm throughout, with few constrictions; accurate horizontal steering is nonetheless important, especially at locations such as the switching magnet at the end of the W line and at injection into RHIC.

Physical Aperture of the AGS to RHIC Transfer Lines

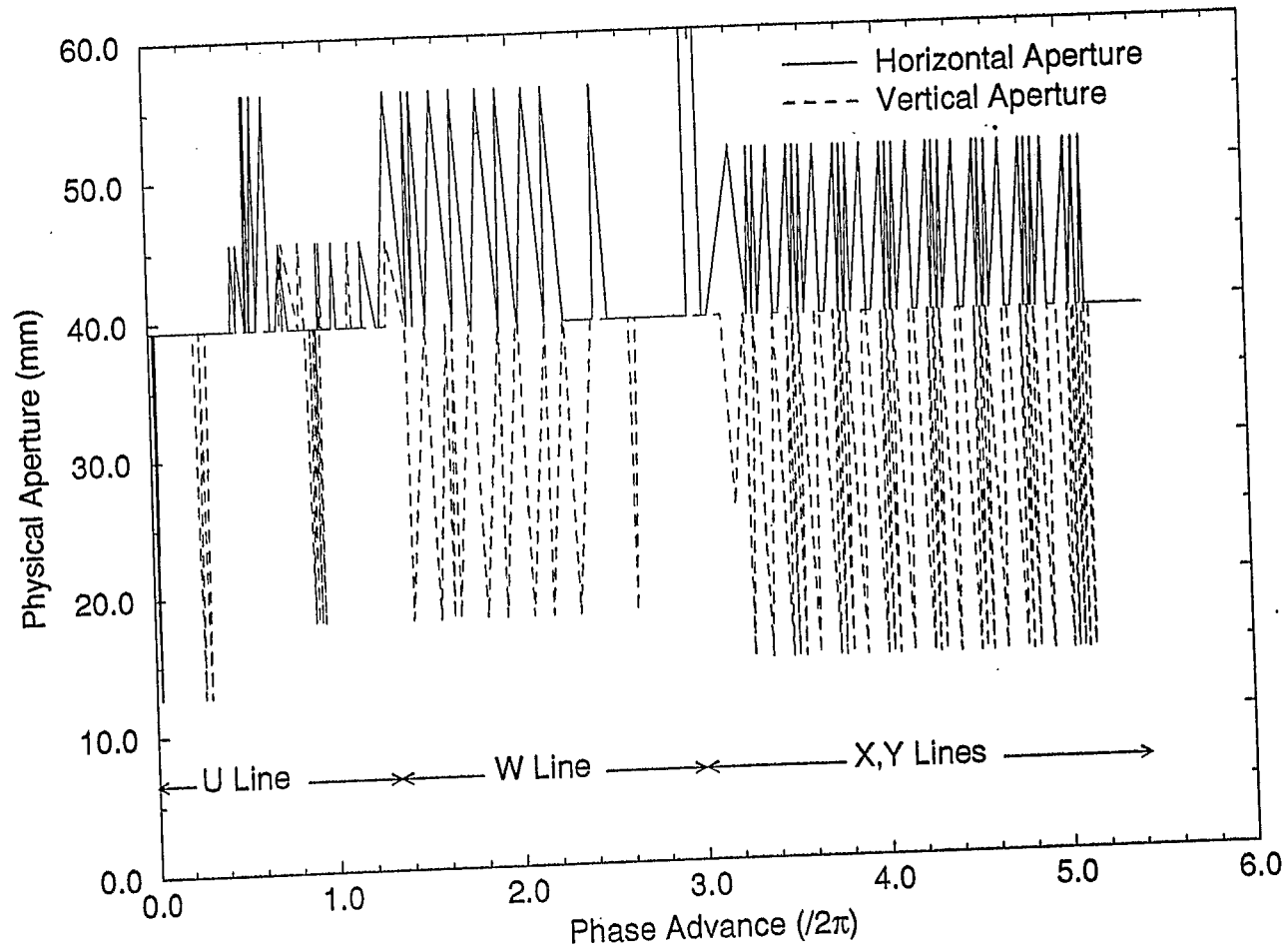


Figure 1: Physical apertures of the AGS to RHIC transfer lines.

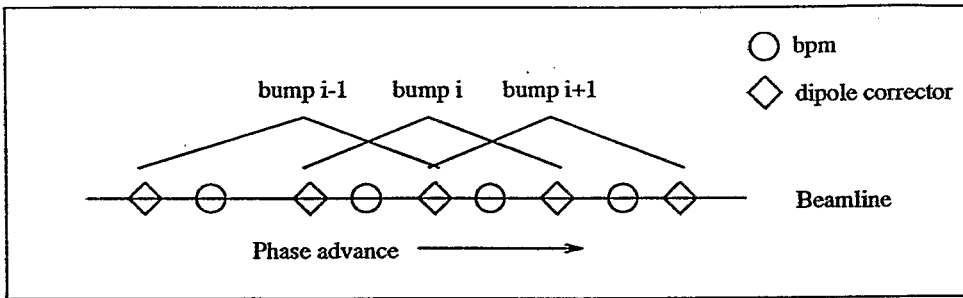


Figure 2: Overlapping 3-bumps in the clorb algorithm.

II. Clorb

Clorb is a general orbit correction routine which uses overlapping 3-bumps and a weighted penalty function to iteratively smooth the linear orbit. Because it does not rely on the specific form of the penalty function (which is traditionally RMS in other approaches), and because it can easily include nonlinear bpm and corrector response, including saturation and power supply limits, clorb is an extremely versatile correction algorithm. Originally used by Peggs et al. at CESR, it is also used in routine operation of the LBL ALS by Lindsay Schachinger and others. This section briefly describes this correction scheme as it will be applied in the AGS to RHIC transfer lines and RHIC.

Clorb is a linear orbit correction program that corrects the orbit based on a given set of position readings (typically BPMs), available dipole correctors and a linear orbit model (beta functions and phase advances). Clorb corrects each transverse plane independently, arranging correctors down the beamline it will correct in groups of three to create overlapping 3-bumps; this overlapping 3-bump layout is shown in Figure 2. For a transfer line this means that clorb corrects orbit displacements only between the first and last correctors — it does not adjust the correctors at the end of the beamline to minimize downstream linear orbit errors, although it can be easily modified to do so. The penalty function of each bump is assessed for the three correctors and all bpm within the range of the bump. The relationship between bpm positions and corrector settings (or the bump strength) is calculated using either measured corrector-bpm response functions, as is done in the ALS, or a linear optics model of the beamline, as is done in this study.

The minimizing procedure of clorb is relatively simple: the penalty function is calculated for a bump and minimized by adjusting the bump strength. This is done in turn for each bump down the beamline and a total penalty function over all bumps is assessed; this procedure is then repeated, starting again with the first bump, until this global penalty

function converges. This iterative approach to orbit correction, using a relatively simple model of the beamline, gives this scheme a robustness not found in other single-pass local-correction approaches. Clorb is not really a local correction algorithm (although it does correct locally) or a global correction algorithm (although it also minimizes a global penalty function) — it is in some sense both. Sets of bpms and correctors may be weighted differently for the penalty function to enforce tighter correction at critical locations; the penalty function may also return large penalties for corrector strengths that are out of range of their power supplies.

In the version of clorb used for AGS to RHIC transfer line orbit correction, a penalty function of the form

$$P = \sum_{i=1}^{N_{\text{bpms}}} B_i (X_i - X_{0,i})^2 + \sum_{j=1}^3 C_j, \quad (2)$$

is used. B represents the bpm weight (1 for used bpms, 0 for broken or unused bpms), X and X_0 are the measured and intended beam positions (in mm), and C is the corrector penalty (1000 for an out of range corrector, 0 for an in range corrector). The units are arbitrary in this penalty function; a bump that needs no further correction has zero penalty. It was found during the course of this study that corrector strengths never saturated for realistic misalignment errors in the AGS to RHIC transfer line, and hence the second term in Equation (2) is negligible here.

Care must be taken to avoid using three-bumps with anomalous distributions of bpms. Monitors that are closer than $\pi/10$ radians in betatron phase to correctors on either end of the three-bump are not used for penalty function calculation in that three-bump — it is presumed such a monitor will be corrected with other bumps. Monitors downstream of the last corrector that are not within any of the three-bumps used by clorb may also be corrected somewhat with the last pair of correctors in the beamline; this was not done in this study, and the deleterious effects of ignoring this correction can be seen in the results described in Section V.

Due to the nature of the design of the AGS to RHIC transfer line, it is important to turn off the corrector 90 degrees upstream of a monitor when it is known that monitor is broken; if this is not done the upstream corrector fight other correctors at unfavorably phased monitors, leading to unusually large corrector strengths and large anomalous bumps at locations without monitors. This approach is taken in Section V when the robustness of the linear orbit correction scheme is tested by turning off individual bpms.

III. Simulations without Randomly Generated Errors

Traditionally all magnetic and misalignment errors in a beamline are generated with random seeds, generating an ensemble of beamlines with “realistic” errors. After correction of each of these random lattices, statistics can be performed on the ensemble to determine the effectiveness of the correction scheme. Here we present an alternative scheme which may be used when the system under investigation is linear (for example, linear coupling and linear orbit correction) and the number of errors to be modeled and corrected is moderately small. This method gives exact results and does not use random seeds, thus eliminating drawbacks such as statistical scalings and sensitivities to anomalous seeds.

It is important to remember that the objective of either approach is to find the one-sigma linear orbit displacement σ_j^{orb} from the design trajectory, given a statistical description of one-sigma linear errors within the beamline. We shall show the equivalence of two approaches to this end. One option is to use an ensemble of N_{seeds} corrected beamlines, with randomly generated errors at all error locations for every beamline from seeds, and calculate the one-sigma linear orbit displacement σ_j^{orb} at any point j . If $x_{j,seed\ i}$ is the j^{th} position in the beamline characterized by seed i , then

$$\sigma_j^{orb} = \lim_{N_{seeds} \rightarrow \infty} \sqrt{\sum_{i=1}^{N_{seeds}} \frac{(x_{j,seed\ i} - \langle x \rangle_j)^2}{N_{seeds}}}, \quad (3)$$

$$\langle x \rangle_j = \frac{1}{N_{seeds}} \sum_{i=1}^{N_{seeds}} x_{j,seed\ i}. \quad (4)$$

Alternatively, we can take an ensemble of N_{errs} corrected beamlines, where N_{errs} is the number of beamline locations with steering errors; each of these beamlines has a single one-sigma error at one of these locations and no steering errors elsewhere. The one-sigma linear orbit displacement is then calculated via

$$\sigma_j^{orb} = \sqrt{\sum_{i=1}^{N_{errs}} (x_{j,error\ i} - \langle x \rangle_j)^2}, \quad (5)$$

$$\langle x \rangle_j = \frac{1}{N_{errs}} \sum_{i=1}^{N_{errs}} x_{j,error\ i}. \quad (6)$$

For errors that do not saturate dipole correctors during the correction procedure, it is reasonable to assume that the correction scheme used by clorb is linear with respect to superposition. That is, if a dipole error $C_{i,1}$ leads to an orbit displacement of $B_{j,1}$ after correction (and the same for a dipole error $C_{i,2}$ and corrected displacement $B_{j,2}$), then a

dipole error $C_{i,1} + C_{i,2}$ will lead to an orbit displacement of $B_{j,1} + B_{j,2}$ after correction. With this assumption, the above formulae can be used to calculate the linear orbit distortion both before and after the correction procedure clorb has been applied.

The equivalence of Equations (5) and (6) to Equations (3) and (4) can be seen from the following reasoning. Because the orbit correction scheme is local, the sums in (5) and (6) for any point x_j in the beamline only carry local contributions; any errors located far upstream or downstream of this point contribute little. This cancellation is performed in (3) and (4) by a phase averaging of many ensembles of errors, all approximately cancelling one another. Since this system is linear with respect to superposition, the averaging performed by taking random beamlines can instead be performed explicitly — we know that errors far away will *exactly* cancel, and the only errors left contributing are local errors. The effect of these local errors can then be summed independently (again assuming superposition) to arrive at Equations (5) and (6).

Therefore, instead of taking the RMS values of the linear orbit over an ensemble of randomly generated (corrected) beamlines, we can take the root of the sum of the squares of 1-sigma orbits (again corrected) over the ensemble of all single 1-sigma errors. There is no scaling by the square root of the number of seeds in the latter, and this method is completely deterministic. These methods are compared in the Section V, where they are found to be in close agreement.

IV. Simulation Procedure and Results

The simulation procedure is diagramed in Figure (3), where processes are represented by lozenges and data are represented by rectangles. Arrows indicate directions of data flow. The machine simulation comprises the left-hand side of the figure, where random dipole errors are simulated; their effects on the orbit are calculated in lorb, a linear orbit simulation module. Lorb gives a simulated linear orbit at *all* elements in the beamline (“God’s linear orbit”) which may be displayed, saved and analyzed.

The central column represents information in the optics database, including information about the lattice layout and elements (in the Lattice SDS) and the beta functions and phase advances between various elements in the lattice (in the Twiss SDS). The linear lattice used in this study is the design lattice, as described in the “Holy Lattice” area used by the RHIC Accelerator Physics group. It is important to note that the optical parameters used are design values, and there is no effort to feed errors or misalignments

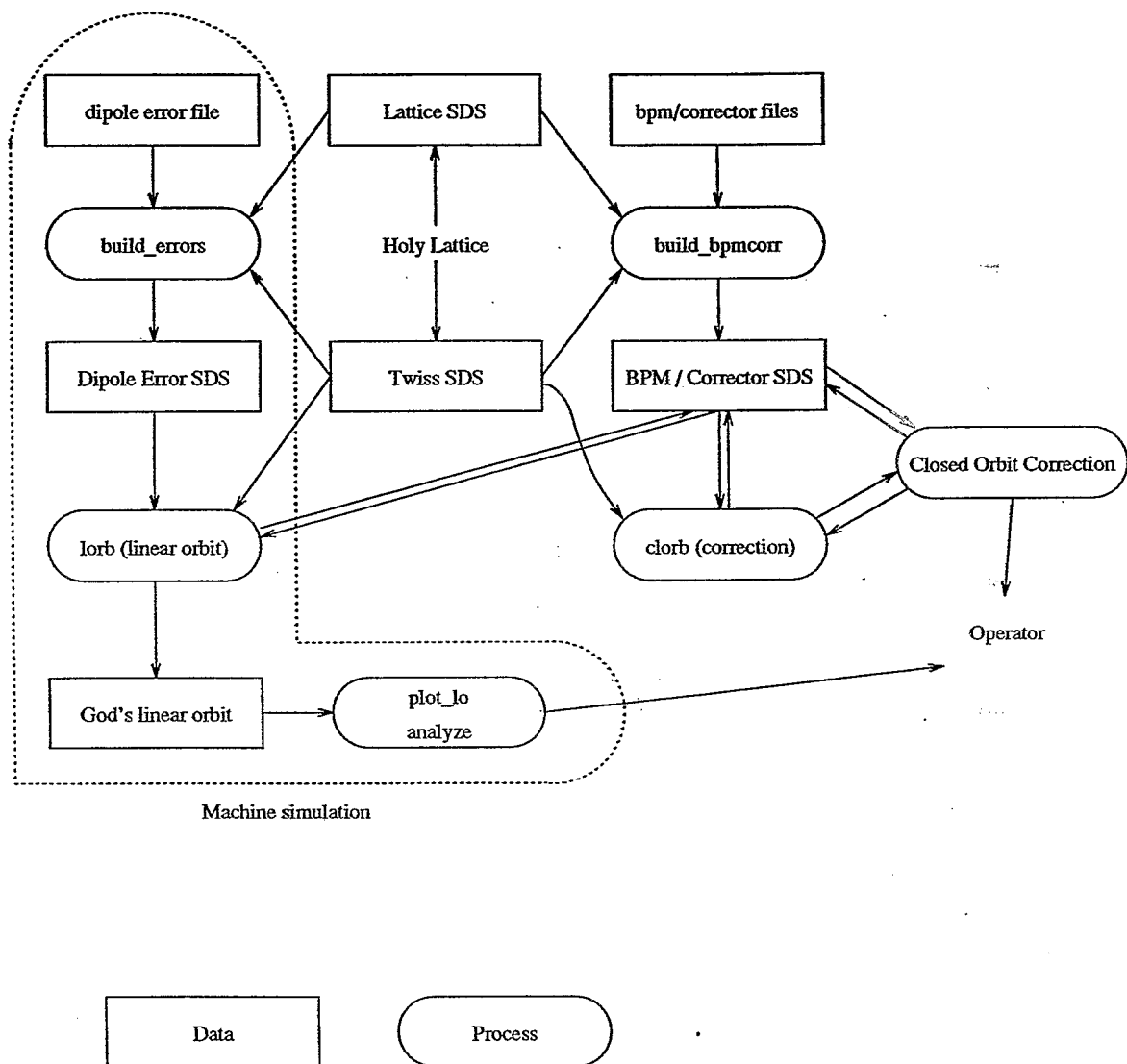


Figure 3: Simulation procedure for AGS to RHIC Transfer Line study, with arrows representing the directions of data flow.

back into this database. Thus this study uses a base design model of the machine plus small well-controlled perturbations from that design.

The left column represents specific information about BPMs and dipole correctors that are used for the orbit correction process. A list of BPMs and correctors to use is retrieved from a file, and data structures are set up in the form of an SDS in shared memory. The simulation of orbit correction is then performed:

- Initialize the BPM and dipole corrector data structures.
- Read the set of dipole errors, either randomly generated from a seed at all misalignment points in the lattice, or a single one-sigma magnet misalignment error as described in the previous section.
- Generate a distorted linear orbit at all BPM locations with `lorb`.
- Use `clorb` to correct this distorted orbit at all BPM locations, using the listed dipole correctors. Typically several runs of `clorb` are necessary here for convergence.
- Use `lorb` to generate a corrected linear orbit at all magnet positions. Store this linear orbit for later analysis.

This procedure allows the simulation of many types of steering error and their correction. There are a variety of sources of these errors, including quadrupole misalignments, dipole rolls, orbit errors in higher order multipoles and differences of actual and design magnet field strengths. In this paper we consider only the first two sources. Nick Tsoupas has recently investigated the last source in the 90 degree bends, based on field variations between new and old steel dipole magnets reported by Peter Wanderer, and found corrector tolerances in this situation to be quite acceptable.

A quadrupole of strength k_1 and length L gives a transverse kick of $\Delta x' = -k_1 L x$; a transverse misalignment of this quad by \bar{x} then gives a steering error of

$$\Delta x'(\text{quad}) = -k_1 L \bar{x} \tag{7}$$

in either dimension. Similarly, the vertical kick from a dipole with bend angle θ rolled by ψ_{roll} around the horizontal axis is approximately

$$\begin{aligned} \Delta x'(\text{dipole}) &= \theta(1 - \cos \psi_{roll}) , \\ \Delta y'(\text{dipole}) &= \theta \sin \psi_{roll} . \end{aligned}$$

This is not strictly correct, but serves as an adequate approximation for this study. Here each dipole was assumed to have an RMS survey roll error of 1.0 mrad, and each quadrupole had an RMS survey transverse displacement of 0.5 mm; these values are somewhat higher than the tolerances expected from survey in these transfer lines.

V. Results and Conclusions

Several tests of correction robustness were applied to the AGS to RHIC transfer lines. First, the misaligned transfer line was simulated using either 20 seeds or 76 single deterministic errors, and the resulting one-sigma orbit displacements were compared. These results are shown in Figures (4) and (5), and there is little noticeable difference between the two methods. Each of these figures also shows the corrector and BPM layout for each plane in the transfer lines (notable is the two-corrector two-BPM pairing design), as well as placement of flags which can be used as surrogate BPMs if necessary for beamline orbit tuning. The similarity of these corrected linear orbits demonstrates that the reasoning in Section III is correct, and an analysis of the beamline orbit correction can proceed without any further reference to seeds, randomly generated errors and statistical weighting.

It is also important to note that in these figures the orbit correction appears to be faulty at a crucial point in the beamline, where the beam goes through the injection lambertson and into RHIC. The lack of correction by clorb in this area was mentioned in Section II, and in the future clorb will be altered to adjust correctors at the end of the transfer line and steer beam properly through the lambertson and injection region.

To test the robustness of the linear orbit correction system against breakdown, single BPMs were broken and the correction then applied to see where additional system redundancy might be required. There are several locations in the transfer lines which might suffer greatly if a single BPM plane were to break — the wbp2/wbp4 pair, the xbp4/xbp5 pair, and xbp3 to name a few. The AGS to RHIC transfer line linear orbit correction system was designed so that the orbit could be completely corrected at several points through the line by pairs of correctors and BPMs placed 90 degrees out of phase.

For completeness, single correctors were also broken to test the correction system. In these circumstances clorb corrected the linear orbit of the beamline nearly as well as with all correctors working, demonstrating that the design of the linear orbit correction system is quite robust when single correctors are broken. There were no correctors in either plane

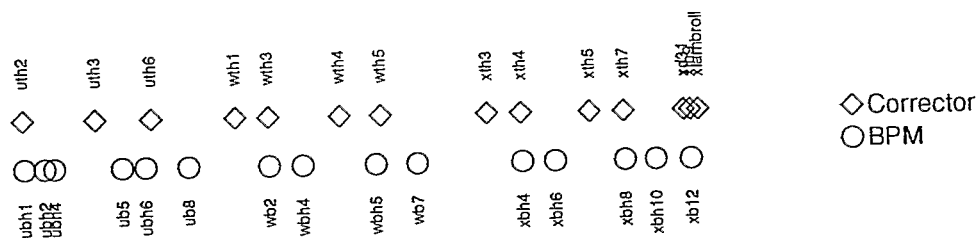
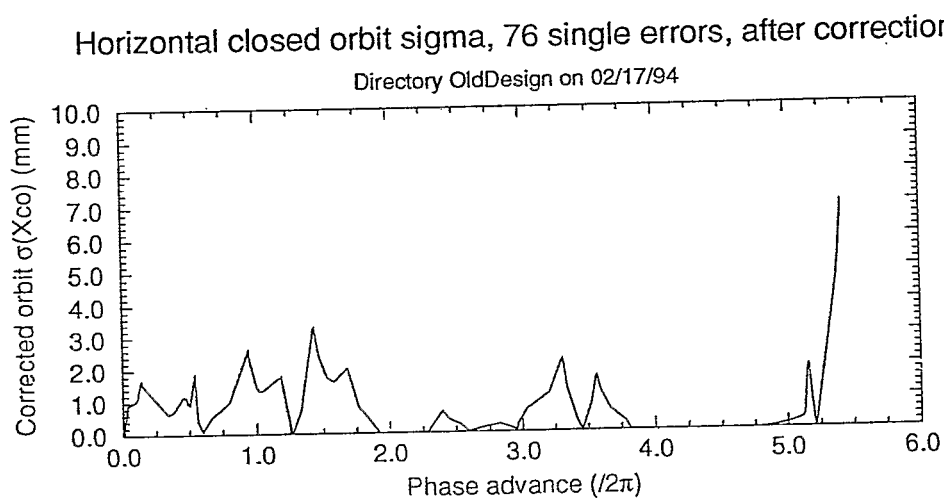
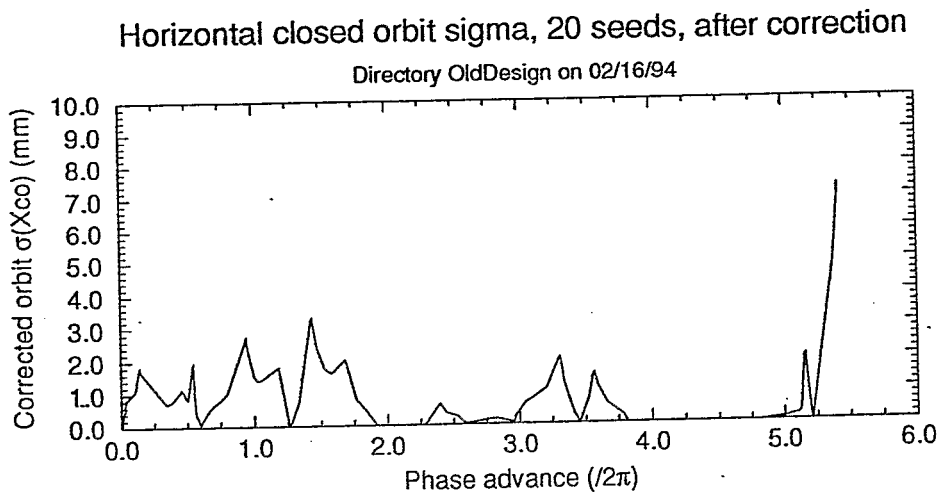


Figure 4: A comparison of horizontal linear orbit correction in the AGS to RHIC transfer line with and without random error seeds. Steering errors are quadrupole misalignments (0.5 mm RMS) and dipole rolls (1.0 mrad RMS).

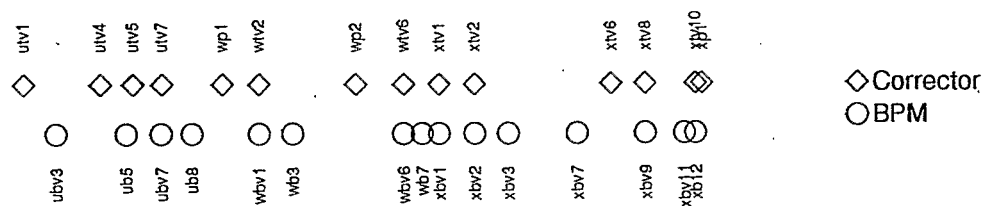
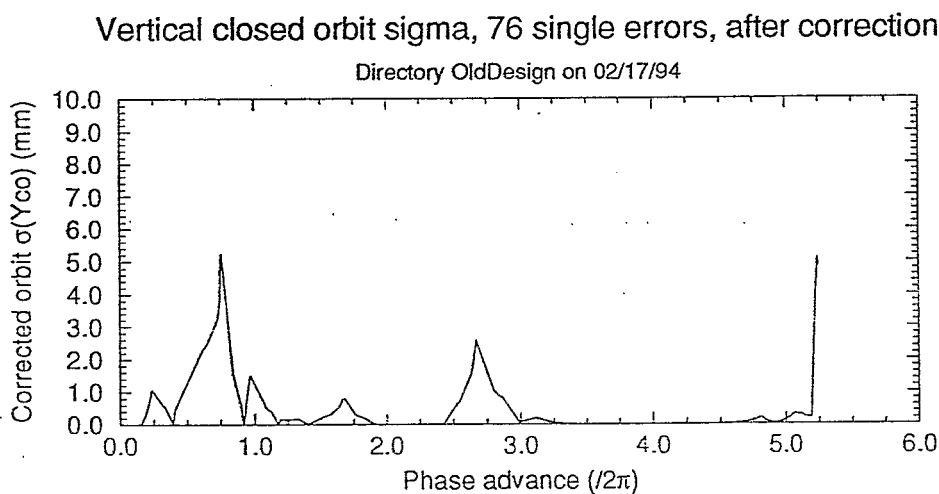
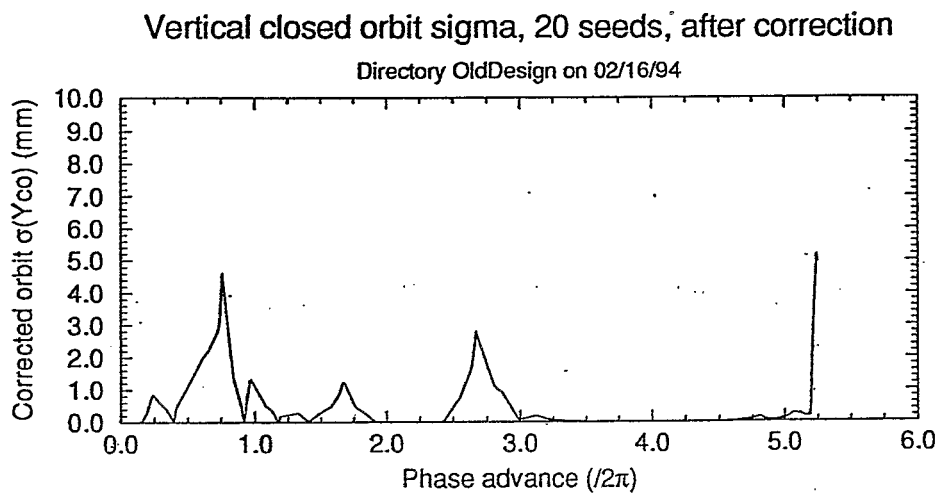


Figure 5: Same as previous figure, for vertical linear orbit correction.

that seemed critical or that led to an unusual inability of the correction system to correct a distorted linear orbit.

In the horizontal plane one critical pair of BPMs are wbp_{mh}2 and wbp_{mh}4, located at horizontal phase advances of approximately 2.00 and 2.25 down the beamline. These BPMs are crucial for correction of upstream steering errors upon entering the W line, and their placement near the end of the 20 degree bend also requires their presence to diagnose any steering problems in this arc. Figure (6) shows that the horizontal orbit errors accumulated over the previous 270 degrees in phase cannot be fully corrected with either one of these BPMs broken, leading to one sigma RMS orbit errors after correction of 10-20 mm. There is no flag nearby for use as a backup position monitor. This area is also of some concern in vertical steering, since the W line contains a vertical drop between pitching magnets wp1 and wp2. Failure of the wbp_{mv}1 BPM plane leads to corrected one sigma RMS orbit errors of up to 15 mm just downstream (Figure 7), within the dipole magnets of the 20 degree bend, so there is also a need for another vertical position monitor in this area.

Another crucial area for orbit correction in both transverse planes is the entry into the X and Y lines, or 90 degree bends. Examining Figures (4) and (5), we see several interesting features. In the horizontal plane, pairs of BPMs are isolated (xbp_{mh}4 and xbp_{mh}5, and xbp_{mh}7 and xbp_{mh}9) without backup readings available. In the vertical plane where the aperture restriction is severe, there is a long region between xbp_{mv}1 and xbp_{mv}8 where several BPMs are placed approximately 180 degrees apart — if xbp_{mv}2 were to break, there would be no information about the phase of the linear orbit that it covered until the end of the arc. The effects on the corrected orbit from each of these BPMs breaking can be seen in Figures (8) through (10); of serious interest is the orbit oscillation in Figure (10) when BPM xbp_{mv}2 is broken, showing that phase coverage of the orbit correction system is insufficient at that point.

For adequate phase coverage at these critical points (through the 20 and 90 degree bends), a rather minimal number of BPM planes can be added. The BPMs wbp_{mh}2 and wbp_{mh}3, previously single-plane, can each be converted to dual-plane BPMs. In this sense each provides phase-redundancy for both BPMs in each plane that bracket them, and allow for full orbit correction even in the event of failure of any single BPM. A dual-plane BPM can also be added in each of the X and Y lines between dipoles D12 and D13. This BPM provides additional horizontal coverage (especially useful considering that horizontal correction may be necessary to compensate for old- and new-steel gradient dipole differences) as well as the phase coverage necessary for redundant correction of the vertical orbit. This

location does not contain any instrumentation or restrictions that would interfere with the installation of an additional dual-plane BPM.

Following is a memo detailing these changes, later implemented by Ted Robinson and Waldo MacKay.

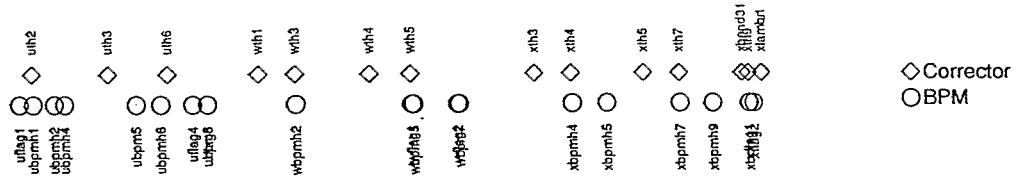
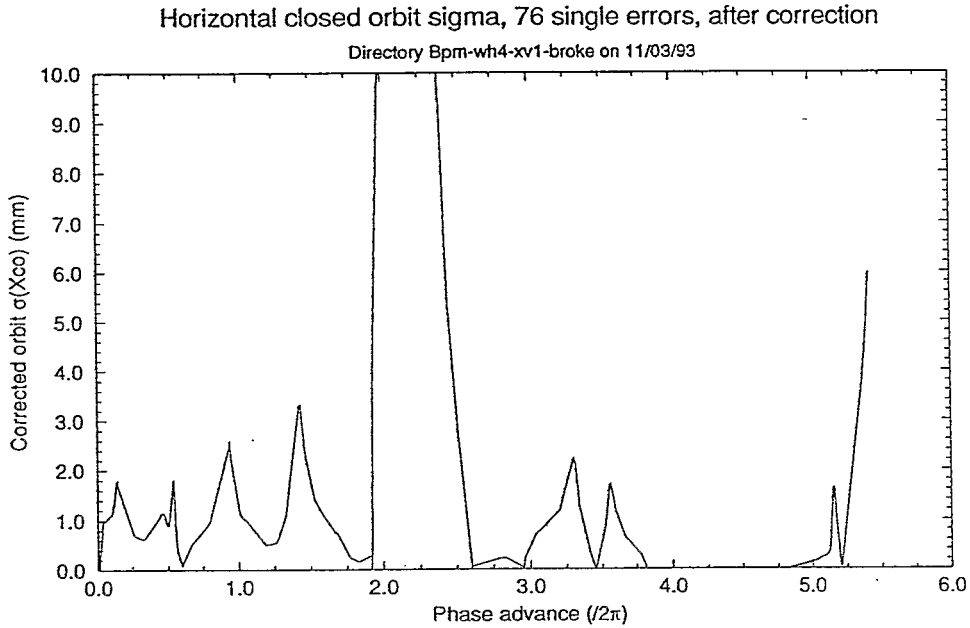
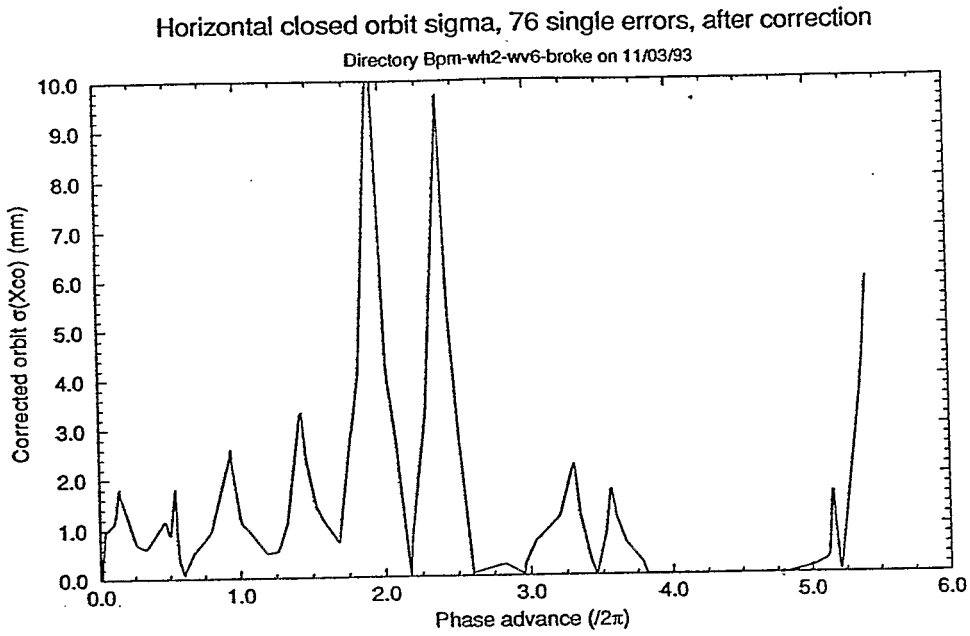


Figure 6: The corrected horizontal linear orbit with BPMs wbpmb2 and wbpmb4 each individually broken.

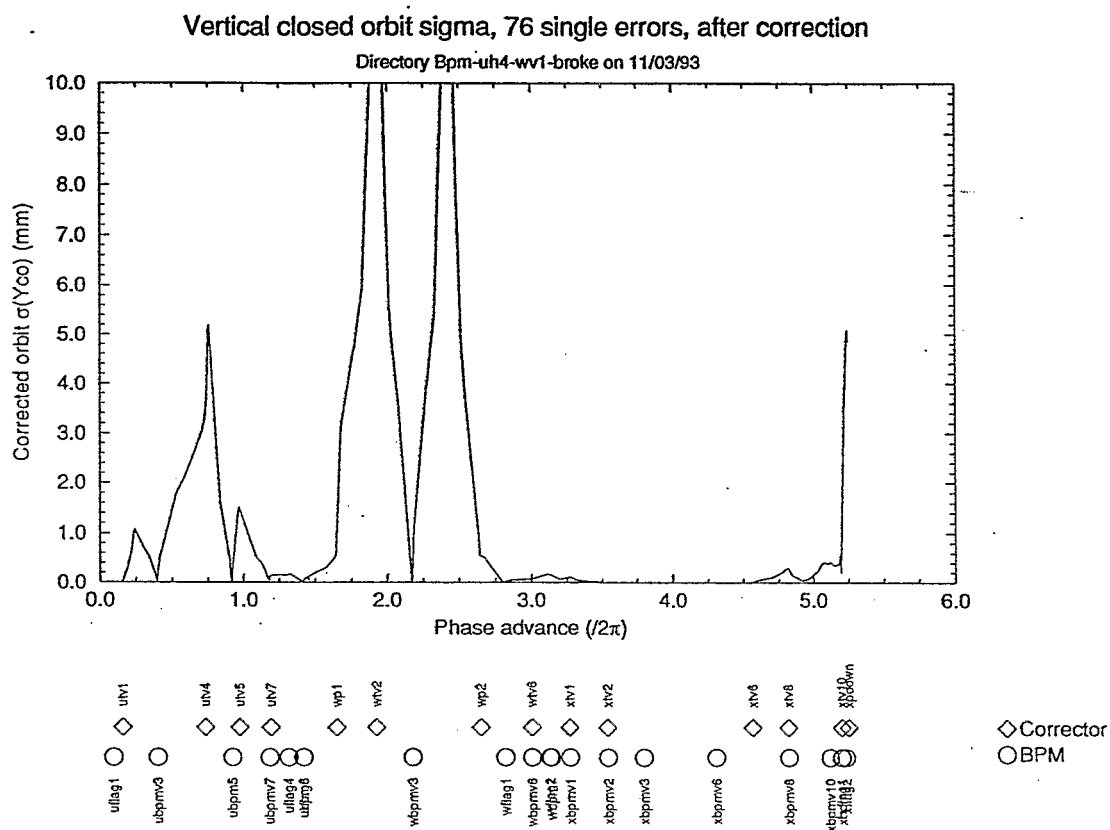


Figure 7: The corrected vertical linear orbit with BPM wbpnv1 broken.

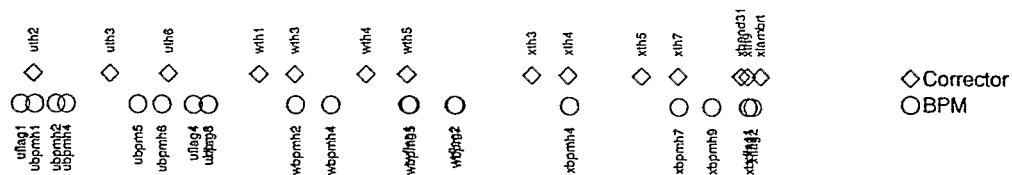
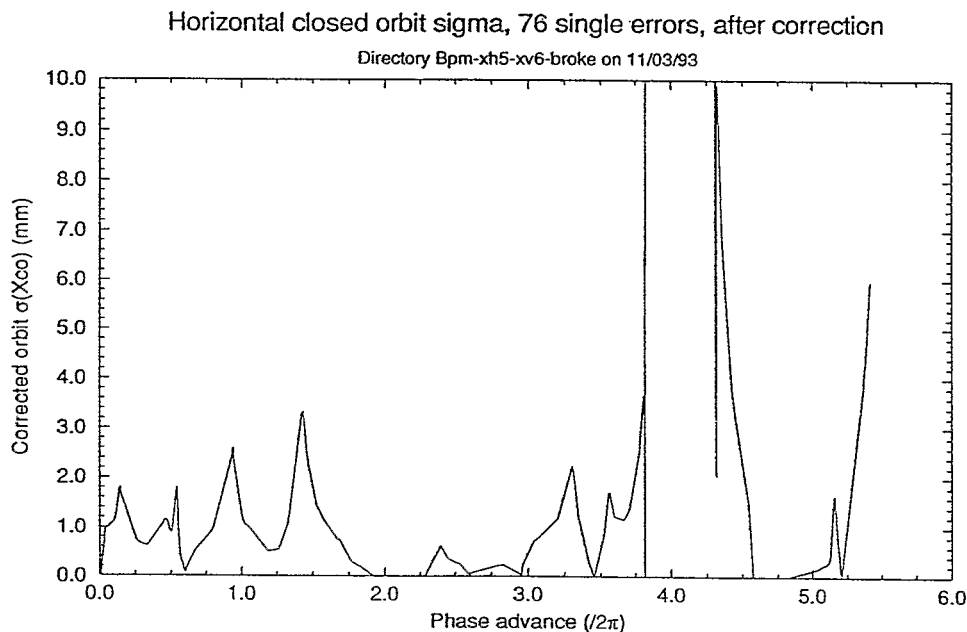
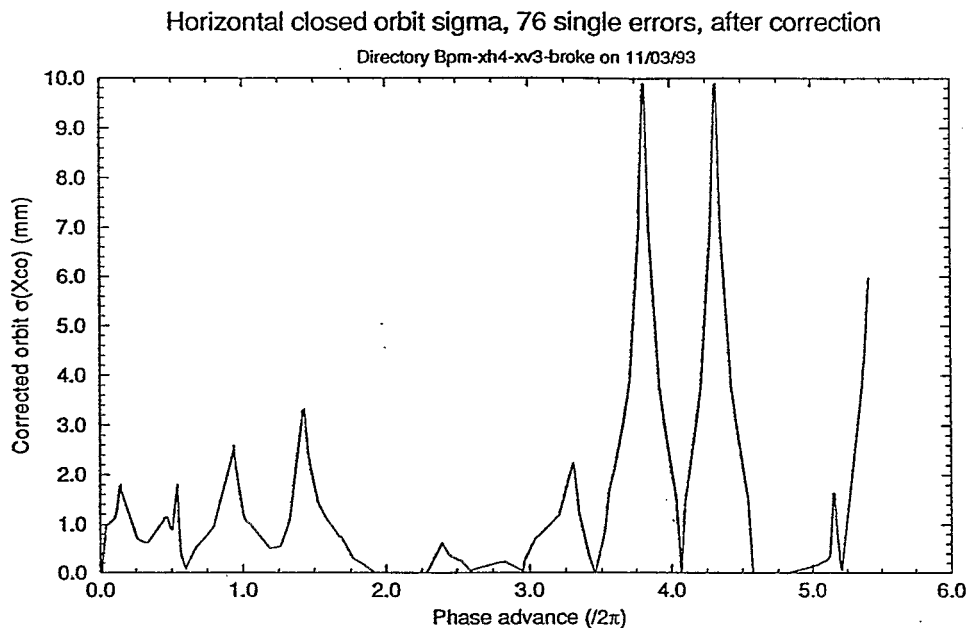


Figure 8: The corrected horizontal linear orbit with BPMs xbpmb4 and xbpmb5 each individually broken.

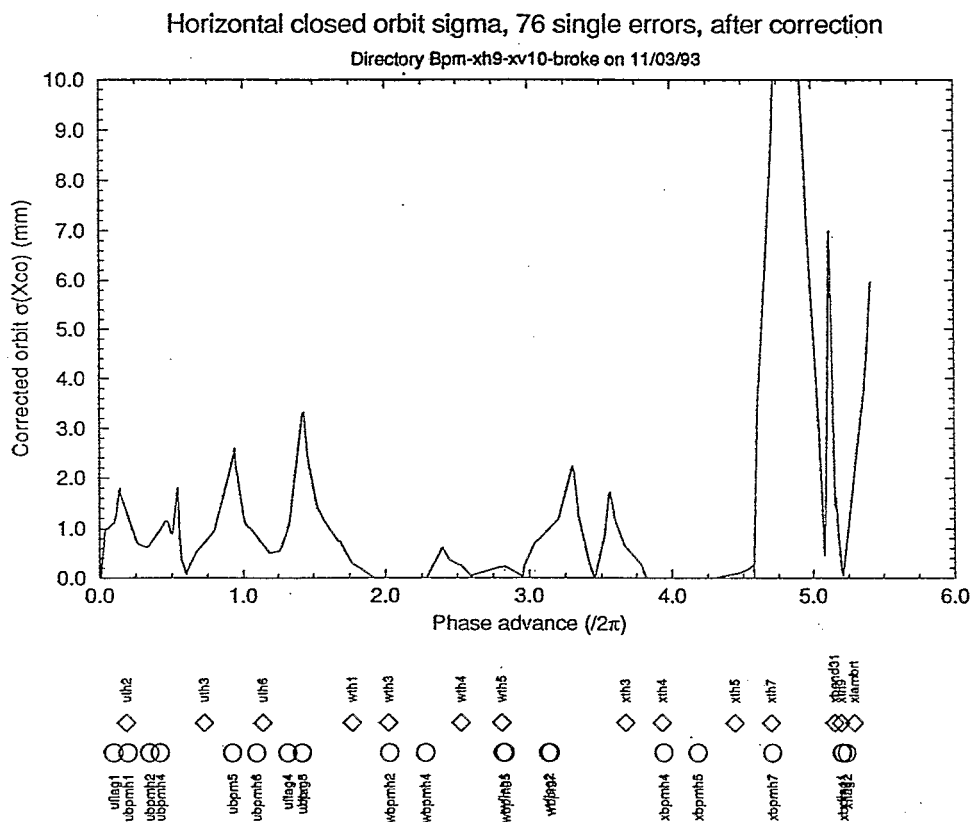
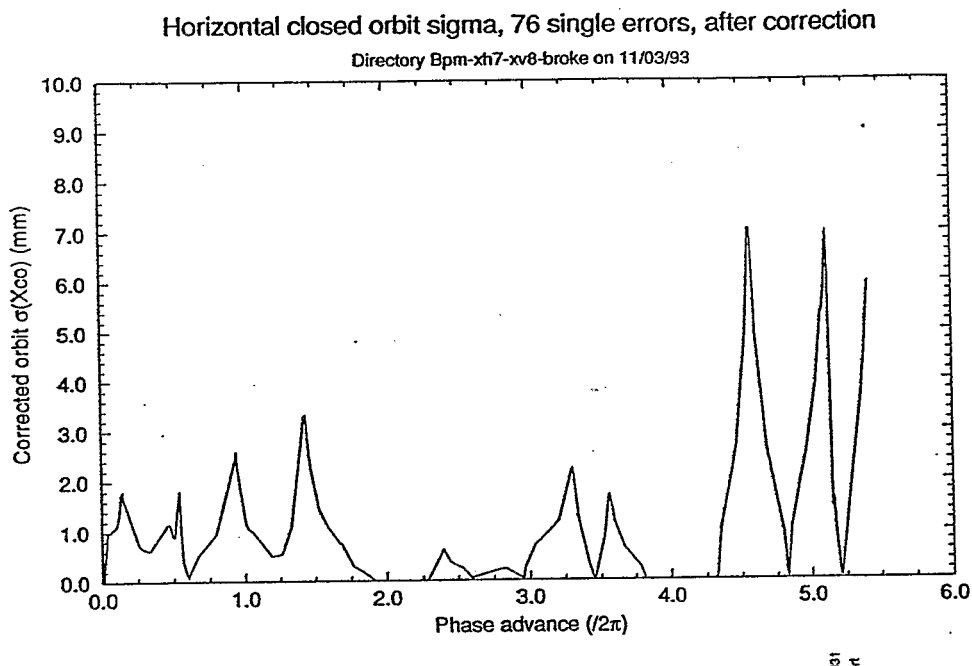


Figure 9: The corrected horizontal linear orbit with BPMs xbpmh7 and xbpmh9 each individually broken.

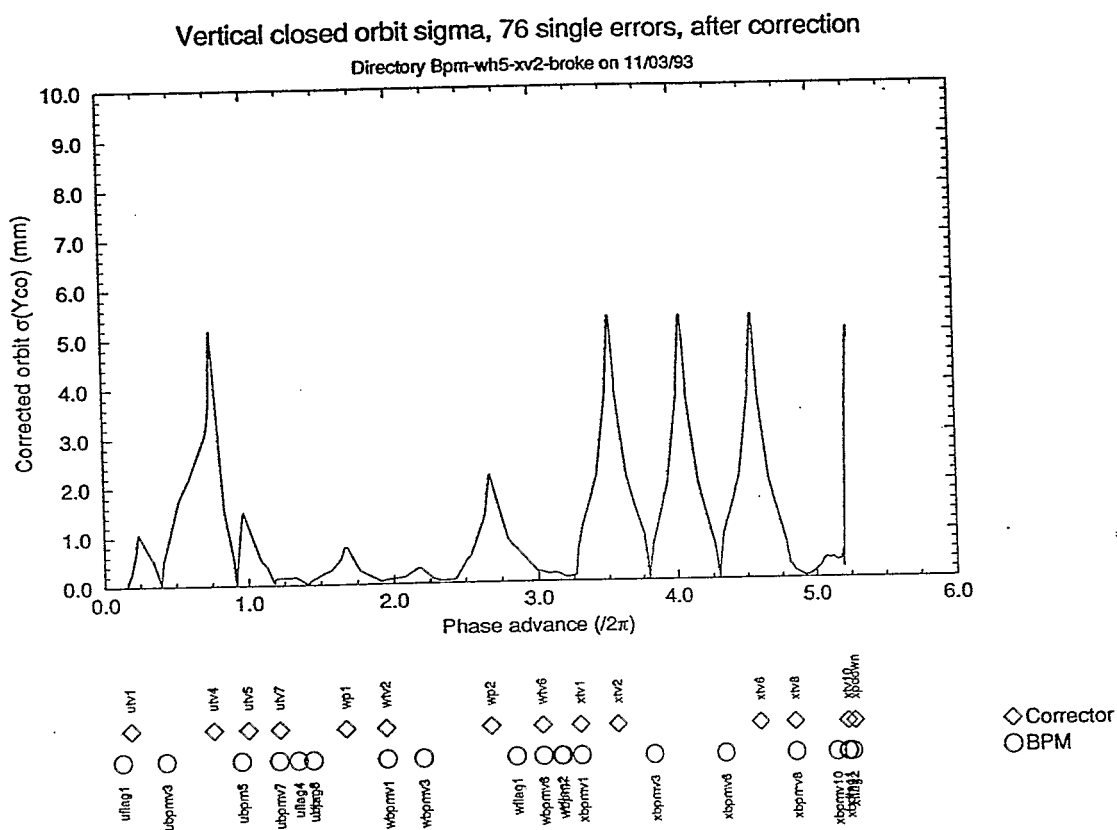


Figure 10: The corrected vertical linear orbit with BPM xbpnv2 broken, showing the orbit oscillation from lack of sufficient phase coverage.

Appendix: Memo detailing BPM layout changes

Changes in BPM layout in the AGS-RHIC Transfer Lines

11/12/93

T. Satogata

To: H. Foelsche, T. Robinson, T. Shea

CC: W. MacKay, S. Peggs, P. Zhou

The current organization of BPMs and dipole correctors in the AGS to RHIC transfer lines has been studied using a linear correction model that will be implemented during the sextant test. A set of typical quadrupole misalignments (feeding down to dipole errors) and dipole roll errors have been used to predict the one-sigma closed orbit after linear orbit correction. This memo details the resulting changes in BPM layout through these transfer lines; there are no changes in the dipole corrector layout, as the current configuration of these elements is adequate.

The criterion for adequate correction of the linear orbit is that, given typical errors, the aperture at all points in the transfer line should be at least 3 sigma of the closed orbit error after correction. This criterion should be met even when any single BPM is broken for adequate redundancy of the correction system. Redundancy of information is also necessary for adequate commissioning of the beamline and controls system, where discrepancies are used to discover errors in installation, and weaknesses and strengths of the design.

The entry into the W line contains a pair of dipole correctors and BPMs in each plane, placed 90 degrees apart in phase advance and designed to fully correct the beam orbit as it enters this region. These pairs are:

Horizontal Correctors: wth1, wth3

Horizontal BPMs: wbpnh2, wbpnh4

Vertical Correctors: wpl, wtv2

Vertical BPMs: wbpnv1, wbpnv3

Failure of any one of these BPMs greatly reduces the effectiveness of orbit correction at this point, in either plane. No flags are nearby for use as backup BPMs, but BPMs wbpmmh2 and wbpmmv3 may be converted to dual-plane BPMs with acceptable phase coverage. Note that this conversion requires no additional vacuum penetrations or change in BPM numbering.

The major aperture restriction of the entire transfer line is the 1.4 cm (radius) vertical aperture in the 90 degree bends (X and Y lines). This following discussion applies to both these bends. The current design for vertical BPM placement in and around the upstream end of these bends has three BPMs placed approximately 180 degrees apart: xbpmmv1, xbpmmv3, and xbpmmv6. These BPMs are redundant, in that each gives essentially the same phase information about the linear orbit. The critical BPM is xbpmmv2, which has no redundant BPM in phase with it until the end of the transfer line. This is unacceptable — failure of this BPM results in a 1-sigma closed orbit error, after correction, of 6-7 mm through the bend.

There is also a lack of redundancy in the horizontal plane in the same region of the 90 degree bends; BPMs xbpmmh4 and xbpmmh5 alone provide orbit information. Both this and the vertical BPM problem are resolved by placing an additional dual-plane BPM in the straight section between dipoles D12 and D13, in both the X and Y lines. At present this straight contains only an ion pump, which will not interfere with the performance of a nearby BPM and which leaves sufficient space for such an installation.

Table 1: BPM placement in AGS-RHIC Transfer Line
As of 11/12/93

Name	plane	s-loc (end)	mu_x	mu_y
ubpmh1	h	5.149	0.014	0.188
ubpmh2	h	16.825	0.040	0.339
ubpmv3	v	33.325	0.119	0.395
ubpmh4	h	37.983	0.147	0.412
ubpm5	hv	88.016	0.566	0.918
ubpmh6	h	112.601	0.938	1.089
ubpmv7	v	124.090	1.005	1.179
ubpm8	hv	159.003	1.262	1.412
wbpmv1	v	230.642	1.773	1.920
wbpmh2	h	248.351	1.922	2.021
wbpmv3	v	266.061	2.022	2.172
wbpmh4	h	283.771	2.172	2.274
wbpmh5	h	348.186	2.601	2.822
wbpmv6	v	368.507	2.801	2.998
wbpm7	hv	389.400	2.955	3.134
xbpmv1	v	403.095	3.056	3.265
xbpmv2	v	425.171	3.447	3.534
xbpmv3	v	443.313	3.688	3.787
xbpmh4	h	453.089	3.817	3.928
xbpmh5	h	471.231	4.067	4.172
xbpmv6	v	480.537	4.194	4.300
xbpmh7	h	508.925	4.577	4.697
xbpmv8	v	518.231	4.713	4.815
xbpmh9	h	526.683	4.825	4.930
xbpmv10	v	543.459	5.085	5.112
xbpm11	hv	561.084	5.211	5.196

ybpmv1	v	403.095	3.056	3.265
ybpmv2	v	425.171	3.447	3.534
ybpmv3	v	443.313	3.688	3.787
ybpmh4	h	453.089	3.817	3.928
ybpmh5	h	471.231	4.067	4.172
ybpmv6	v	480.537	4.194	4.300
ybpmh7	h	508.925	4.577	4.697
ybpmv8	v	518.231	4.713	4.815
ybpmh9	h	526.683	4.825	4.930
ybpmv10	v	543.459	5.085	5.112
ybpm11	hv	561.084	5.211	5.196

Table 2: BPM placement in AGS-RHIC Transfer Line

Additions and changes

11/12/93

Name	plane	s-loc (end)	mu_x	mu_y
ubpmh1	h	5.149	0.014	0.188
ubpmh2	h	16.825	0.040	0.339
ubpmv3	v	33.325	0.119	0.395
ubpmh4	h	37.983	0.147	0.412
ubpm5	hv	88.016	0.566	0.918
ubpmh6	h	112.601	0.938	1.089
ubpmv7	v	124.090	1.005	1.179
ubpm8	hv	159.003	1.262	1.412
wbpmv1	v	230.642	1.773	1.920
wbpm2	hv	248.351	1.922	2.021 <-- change from H to dual
wbpm3	hv	266.061	2.022	2.172 <-- change from V to dual
wbpmh4	h	283.771	2.172	2.274
wbpmh5	h	348.186	2.601	2.822
wbpmv6	v	368.507	2.801	2.998
wbpm7	hv	389.400	2.955	3.134
xbpmv1	v	403.095	3.056	3.265
xbpmv2	v	425.171	3.447	3.534
xbpmv3	v	443.313	3.688	3.787
xbpmh4	h	453.089	3.817	3.928
xbpm5	hv	462.155	3.980	4.058 <-- added dual plane
xbpmh6	h	471.231	4.067	4.172
xbpmv7	v	480.537	4.194	4.300
xbpmh8	h	508.925	4.577	4.697
xbpmv9	v	518.231	4.713	4.815
xbpmh10	h	526.683	4.825	4.930

xbpmv11	v	543.459	5.085	5.112	
xbpm12	hv	561.084	5.211	5.196	
ybpmv1	v	403.095	3.056	3.265	
ybpmv2	v	425.171	3.447	3.534	
ybpmv3	v	443.313	3.688	3.787	
ybpmh4	h	453.089	3.817	3.928	
ybpm5	hv	462.155	3.980	4.058	<-- added dual plane
ybpmh6	h	471.231	4.067	4.172	
ybpmv7	v	480.537	4.194	4.300	
ybpmh8	h	508.925	4.577	4.697	
ybpmv9	v	518.231	4.713	4.815	
ybpmh10	h	526.683	4.825	4.930	
ybpmv11	v	543.459	5.085	5.112	
ybpm12	hv	561.084	5.211	5.196	